RSC Advances

ROYAL SOCIETY OF CHEMISTRY

PAPER

View Article Online
View Journal | View Issue

Cite this: *RSC Adv.*, 2020, **10**, 40068

Stimuli-responsive gelators from carbamoyl sugar derivatives and their responses to metal ions and tetrabutylammonium salts†

Dan Wang, Anji Chen, ‡ Joedian Morris and Guijun Wang *

Received 4th September 2020
Accepted 7th October 2020

DOI: 10.1039/d0ra07587f

rsc.li/rsc-advances

Carbohydrate-based low molecular weight gelators (LMWGs) are interesting compounds with a variety of applications. In this research, a library of nineteen carbamate derivatives of *N*-acetyl-D-glucosamine were synthesized and characterized, and several derivatives were found to be effective LMWGs. They formed gels in pump oils as well as mixtures of water with ethanol or water with DMSO. The structures of the carbamoyl chains played an important role in the gelation properties, short chain aliphatic derivatives and phenyl carbamates formed gels in more solvents than certain aromatic and dimeric carbamates. The phenyl carbamate gelator was also selected for the encapsulation of naproxen sodium, and the drug slowly diffused from the gel to the aqueous phase as indicated by UV-vis spectroscopy. In addition, we also found that the *p*-methoxyl benzyl carbamate derivative showed interesting stimuli-responsive gelation properties in the presence of metal salts and tetrabutylammonium salts. The gels were characterized using optical microscopy, scanning electron microscopy, rheology and other methods. The self-assembling mechanisms of the gelators were studied using ^{1}H NMR spectroscopy. The preparation, characterization, and molecular assembling properties of these compounds are reported. The results obtained from this study are useful for the design of other LMWGs and the sugar derivatives can be explored for different biological applications. The formation of spontaneous ionic gels can be applicable for a plethora of applications including catalysis and environmental remediation.

Introduction

Supramolecular gelation through low molecular weight gelators (LMWGs) has gained much attention over recent years. Several classes of LMWGs have been reported, depending on the solvents used, these include both hydrogelators and organogelators.[1–6] They have been explored for applications in many research fields including drug delivery and tissue engineering,[7–9] as catalysts for organic reactions,[10] as well as in environmental applications to remove pollutants.[11,12] The structure-based approach can allow for the design and discovery of supramolecular gelators with desirable functions. For instance, stimuli-responsive gelators have been studied for their unique and controllable properties.[13–18] Metallogels and ionogels are useful soft materials with a variety of applications ranging from anion sensing and catalysis to electrochemical applications.[19–22] Ionogels formed by gelators in ionic liquids or salts have been investigated for their potential applications in dye sensitized solar cells. Anion binding and anion-responsive molecular gelators can function as host–guest receptors, making them useful for anion sensing.[23–26] Gels responsive to anions and cations may have distinctive properties to function as sensors and may also be beneficial for catalysis.[20,27–32]

Carbohydrate derived low molecular weight gelators are intriguing compounds with many potential applications.[5,33–35] Several organogelators and hydrogelators have been obtained by selectively functionalizing the different hydroxyl groups from common monosaccharides such as D-glucose and D-glucosamine.[36] Among the functional groups that are effective for molecular gelators, amide, carbamate, and urea functions have been shown to be efficient in the formation of supramolecular gels.[37–40] Some bis-arylcarbamate derivatives[38] as well as carbamoyl functionalized glucose and glucosamine derivatives were reported as LMWGs.[39,40] Amides based gelators have been used as anion binding agents and they played a significant role in molecular recognition.[19] Several amide based derivatives have shown susceptibility towards anion stimuli.[41] A glucose-based gelator formed gels in tetramethyl ammonium bromide electrolyte solution, the resulting ionogels showed thermal

---

Department of Chemistry and Biochemistry, Old Dominion University, 4541 Hampton Boulevard, Norfolk, VA 23529-0126, USA. E-mail: g1wang@odu.edu; Fax: +1 757 683 4628; Tel: +1 757 683 3781

† Electronic supplementary information (ESI) available: Gelation properties in tetramethylammonium bromide and tetrabutylammonium salts, stability of the gels in basic conditions, NMR spectra for compounds **13** and **20** at different temperatures; NMR studies of compounds **18** and **20** with different amount of TBABr, additional gel photos for naproxen. The ^{1}H and ^{13}C NMR spectra of all intermediates and final products are provided. See DOI: 10.1039/d0ra07587f

‡ Current address: TCG GreenChem, Inc. 737 North 5th Street, Suite 501, Richmond, VA 23219, USA.

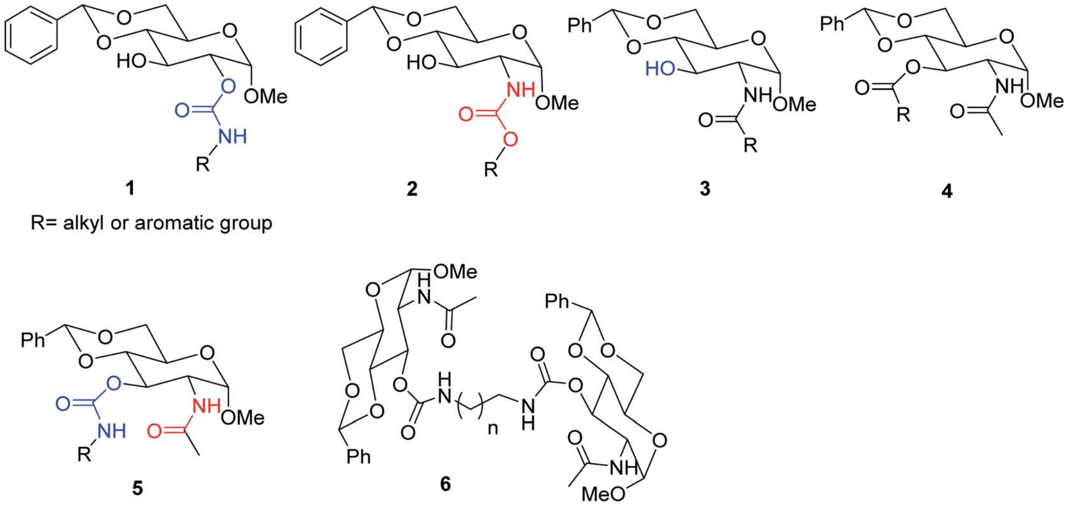

Fig. 1 Structures of several classes of sugar derivatives that can function as effective LMWGs (**1–4**) and the compounds synthesized in this study (**5–6**).

reversibility and enhanced conductivity.[42] Two glycolipid derived gelators were shown to be fluoride responsive.[43] Organic carbamate or urethane derivatives have played important roles in the design and study of low molecular weight gelators (LMWGs).[38,40,44–46] The carbamate functional group contains one hydrogen bonding donor (NH) and two hydrogen bonding acceptors (N and O), therefore they can form intermolecular hydrogen bonding networks among the gelators and also with solvent molecules. In comparison to amides, carbamates contain an extra hydrogen bond acceptor which may play an important role in molecular self-assemblies and the interaction with other atoms.

During the course of the functionalization of monosaccharide derivatives to produce effective supramolecular assemblies and advanced functional biomaterials; certain correlations between the structures of the compounds and their gelation properties have been established.[40,47–50] As shown in Fig. 1, the various C-2 acylated derivatives of 4,6-*O*-benzylidene acetal protected D-glucosamine derivatives have proven to be effective low molecular weight gelators (LMWGs). These include the D-glucose derived carbamate **1**, D-glucosamine derived carbamate **2**,[40] and D-glucosamine derived amide **3**. Recently, we demonstrated that the 3-*O*-esters of glucosamine derivatives **4** were also effective gelators.[47] These compounds were typically synthesized in a few steps from *N*-acetyl-D-glucosamine (NAG).[49] Based on the interesting gelation results from the 3-ester derivatives, we envisioned that the isosteric carbamate derivatives at the 3-OH position may result in another class of effective gelators with the general structure **5**. Previously, we have demonstrated that the replacement of an ester with a carbamate functional group by introducing the NH hydrogen bonding donor enhanced gelation properties of the sugar derivatives.[40] The new carbamate derivatives **5** have several desirable features that will lead to a new class of organogelators. It contains an acetamide functional group at the C-2 position, which can also contribute to intermolecular hydrogen bonding. The carbamate derivatives are more stable at basic conditions in comparison to the corresponding ester analogs, therefore, for certain applications where stable gelators are desirable, the carbamates would be suitable. In this research, in order to probe the structural influence of sugar derivatives towards molecular self-assemblies and discover novel functional supramolecular gelators, we introduced carbamoyl functional groups to the 3-OH position of a 4,6-*O*-benzylidene acetal protected *N*-acetyl-D-glucosamine derivative. A series of carbamate derivatives with the general structures **5** and the dimeric carbamates **6** were synthesized and analyzed.

Results and discussions

As shown in Scheme 1, carbamate derivatives **9–27** were synthesized and characterized. Two methods were used for the preparation of the compound libraries. Compounds **12–14**, **16–17** and **20–23**, were prepared by following the methods reported previously using commercially available isocyanates.[51] The others, including compounds **9–11**, **15**, **18–19**, and the biscarbamates **24–27** were synthesized using the imidazole carbonate intermediate **8** by reacting with different amines. Carbonyl di-imidazole (CDI) has been used often for the formation of cyclic carbamates from vicinal amino alcohol or linear carbamate by stepwise acylation reactions. The sugar alcohol **7** was treated with CDI first to form the corresponding imidazole carboxylate **8** effectively, this intermediate reacted readily with primary amines to produce the desired carbamates. When using α, ω-diamines, four different dicarbamate derivatives were synthesized successfully as shown in Scheme 1.

Gelation properties

After these compounds were synthesized and purified, their gelation properties were tested in a panel of organic solvents and aqueous solutions, the results are shown in Table 1. All compounds were insoluble in hexane, whilst most were

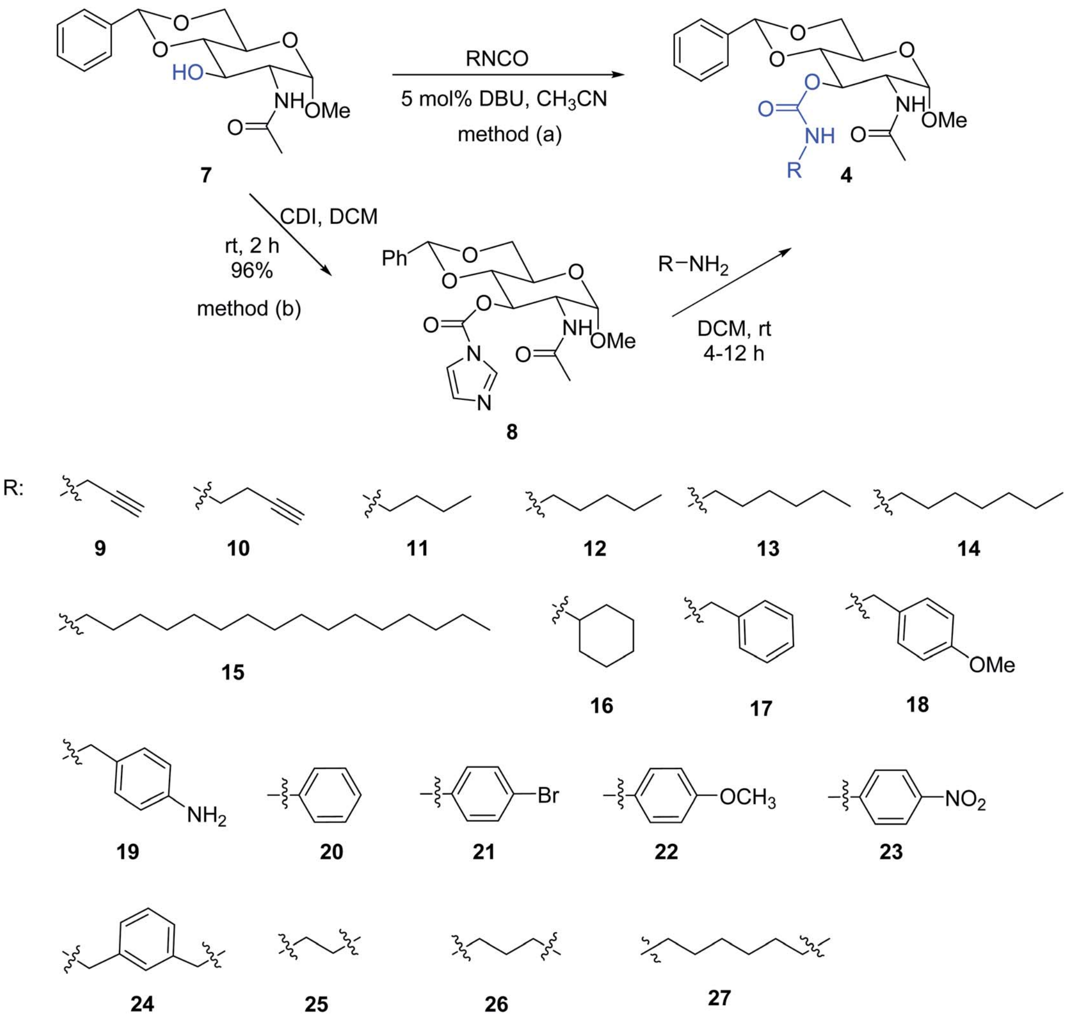

Scheme 1 Synthesis of monomeric 3-*O*-carbamate derivatives **9–23** and dimeric derivatives **24–27**.

insoluble in water except compounds **10** and **19**, which formed partial gels at 20.0 and 6.7 mg mL^{-1}, respectively. The short chain aliphatic carbamate derivatives showed similar gelation tendencies to the corresponding ester derivatives with the same alkyl chain. These compounds showed effective gelation properties for DMSO/water or ethanol/water mixtures. However, the aromatic derivatives were less effective gelators.

The linear aliphatic carbamate derivatives formed gels in pump oil, with the five carbon to seven carbon (compounds **12–14**) being the most efficient; forming gels at lower MGCs in pump oil in comparison to the others. The hexyl carbamate derivative **13** was the most versatile gelator among the alkyl derivatives, forming gels in six of the selected solvents. The very long chain derivative **15** only formed gels in pump oil but not in the other selected solvents, the compound contains a very long chain fatty acyl group which increases the hydrophobic interactions and van der Waals forces significantly. The cyclohexyl derivative **16** formed gels in ethanol/water mixtures and DMSO/water (1 : 1) mixture, similarly to the short chain linear carbamates but at lower MGCs. For the aromatic derivatives, the benzyl derivative **17** showed good gelation properties in ethanol/water mixtures and DMSO/water mixtures, the *p*-methoxy benzyl carbamate **18** and the phenyl carbamate **20** were the most versatile gelators among all the compounds synthesized in this study, forming gels in eight different solvents. Interestingly, the substituted phenyl derivatives were not effective gelators as most of them were insoluble in the tested solvents. Several dimeric bis-polar carbamate derivatives were also synthesized but these compounds did not form gels in most of the tested solvents, except that compounds **24** and **26** formed gels in pump oil and **24** formed a gel in DMSO/H_2O (v/v 1 : 2). The dimeric carbamates with two opposing sugar headgroups have intense intermolecular interactions which result in stronger packing therefore becoming insoluble or forming a precipitate.

Many carbamate derivatives formed stable gels in the DMSO and water mixture although not in pure water. To find out the minimum amount of DMSO required for gelation in aqueous solutions, the gelation properties of compounds **18** and **20** were tested in different ratios of DMSO and water, the results are shown in Table 2. These two most versatile gelators formed gels at

Table 1 Gelation properties of the carbamate derivatives[a]

No.	Structures of R:	Pump oil	Tol	i-PrOH	EtOH	EG	Glycerol	H_2O	EtOH : H_2O (1 : 1)	EtOH : H_2O (1 : 2)	DMSO : H_2O (1 : 1)	DMSO : H_2O (1 : 2)
9	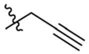	P	G_P	P	P	P	G_O 20.0	I	P	P	P	G_O 20.0
10	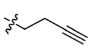	G_T 20.0	S	P	P	P	P	G_P	G_P	G_P	P	G_P
11	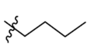	G_T 20.0	S	P	S	G_O 20.0	G_T 20.0	P	G_P	G_P	G_O 20.0	G_O 20.0
12	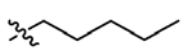	G_O 10.0	Go 20.0	S	S	P	I	I	G_T 20.0	G_O 20.0	G_O 10.0	P
13	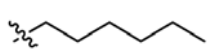	G_O 5.0	S	S	S	P	G_O 20.0	I	G_O 10.0	G_O 10.0	G_O 20.0	G_O 20.0
14	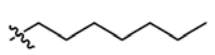	G_O 5.0	S	S	S	G_O 10.0	I	I	G_O 10.0	G_O 5.0	G_O 10.0	I
15	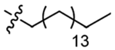	G_T 5.0	P	P	P	G_P	S	P	P	P	P	I
16	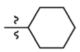	I	S	S	S	I	S	I	G_O 5.0	G_O 3.3	G_O 6.7	I
17	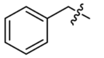	I	G_C 20.0	P	P	S	P	I	G_O 2.5	G_O 2.5	G_O 10.0	G_O 10.0
18	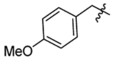	G_T 20.0	P	G_O 10.0	P	G_O 10.0	G_C 6.7	I	G_O 4.0	G_O 10.0	G_O 2.5	G_O 3.3
19	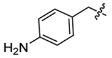	P	I	S	P	S	S	G_P 6.7	S	G_P	S	S
20	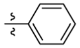	I	G_O 2.8	G_C 10.0	G_C 20.0	P	G_O 20.0	I	G_O 3.3	G_O 2.5	Go 4.0	G_O 2.8
21	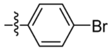	I	G_C 20.0	P	P	P	P	I	I	I	P	P
22	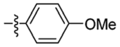	I	P	P	P	P	I	I	I	P	P	P
23	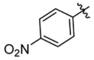	I	P	S	S	P	I	I	P	P	P	P
24	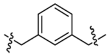	G_T 20.0	I	I	G_P	P	S	I	G_P	G_P	P	G_T 6.7
25	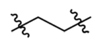	I	I	G_P	G_P	G_T 20.0	I	I	G_P	P	I	G_P
26		G_T 10.0	G_P	P	P	P	S	I	I	I	P	P
27	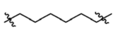	I	G_P	G_P	P	P	S	I	I	I	P	I

[a] G, gel at room temperature, the numbers are the corresponding minimum gelation concentrations (MGCs) in mg mL^{-1}; G_C, clear or transparent gel; G_T, translucent gel; G_O, opaque gel; G_P, partial gel at 20 mg mL^{-1} unless otherwise specified; I, insoluble; P, crystallize or precipitate; S, soluble at ~20 mg mL^{-1}.

Table 2 Gelation test in DMSO water mixture for compounds **18** and **20**[a]

	DMSO : H_2O volume ratio									
Compound	1 : 0	1 : 1	1 : 2	1 : 3	1 : 4	1 : 5	1 : 6	1 : 7	1 : 8	1 : 9
18	S	G_T 10.0	G_T 6.7	G_T 5.0	G_T 4.0	G_T 3.3	G_T 2.8	G_T 2.5	G_T 2.2	P
20	S	G_O 10.0	G_O 6.7	G_O 5.0	G_O 4.0	G_O 3.3	G_O 2.8	G_O 2.5	G_O 2.2	G_O 2.0

[a] G, gel formed after heating; S, soluble; P, precipitation. G_T, translucent gel, G_O, opaque gel. The numbers following the letters are the concentrations in mg mL^{-1} of the solvent mixture.

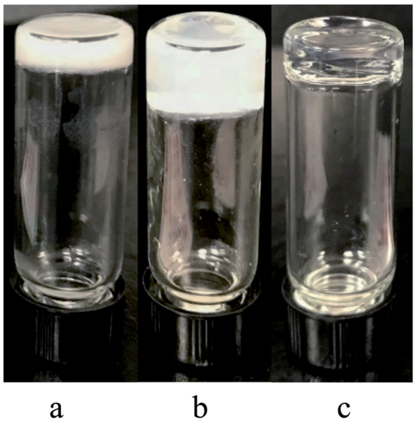

Fig. 2 (a) An opaque gel formed by compound **13** in EtOH/H_2O (v/v 1 : 1) at 10 mg mL^{-1}; (b) an opaque gel formed by compound **17** in EtOH/H_2O (v/v 1 : 2) at 2.5 mg mL^{-1}; (c) a transparent gel formed by compound **20** in i-PrOH at 10.0 mg mL^{-1}.

different ratios of DMSO with water from 1 : 1 up to 1 : 9. Most of the gels appeared opaque, while some were translucent or transparent. A few representative examples are included in Fig. 2.

Further gelation properties of compound 18 for different metal ions

To further explore the potential applications of these sugar based gelators, the properties of these compounds were further evaluated. The *p*-methoxyl benzyl compound **18** was selected as the sample gelator since it formed stable gels in most solvents. This compound was tested for gelation in the presence of several earth-abundant metals including $Hg(OAc)_2$, $Ni(OAc)_2$, $Zn(OAc)_2 \cdot 2H_2O$, $Cu(OAc)_2$, $Pb(OAc)_4$, and $FeCl_2$. The gelation test was performed by the standard heating and cooling method and several salts were able to form homogenous stable gels. The tests were then repeated by mixing the metal ion solutions with the gelator solution to observe whether the gels can form spontaneously without heating. The compound **18** was dissolved in DMSO first, addition of an equal volume of the aqueous metal salt solution to the gelator solution resulted in spontaneous gelation for several metal salts. The gel photos are shown in Fig. 3.

For samples in biomimetic environments and for potential biomedical applications, it is desirable to form hydrogels with minimum amount of DMSO. We analyzed the gelation properties of compound **18** for several biologically relevant metal ions such as Ca^{2+}, Zn^{2+}, Fe^{3+}, Cu^{2+}, and vitamin B_2. Spontaneous gels were formed by simply adding the aqueous solutions of the metal ions to the compound **18** solution at room temperature, these are shown in Fig. 4. The metal salts used are (a) $Cu(OAc)_2 \cdot H_2O$, (b) $FeCl_3$, (c) $Zn(OAc)_2 \cdot 2H_2O$, (d) $CaO_3PO(CH_2)_2N(Cl)(CH_3)_3 \cdot 4H_2O$. Vitamin B_2 co-gels are shown in Fig. 4e and f.

Gel characterizations

The gel morphology was characterized using optical microscopy and scanning electron microscopy. Some examples of these micrographs are included in Fig. 5 and 6. The gel formed by the

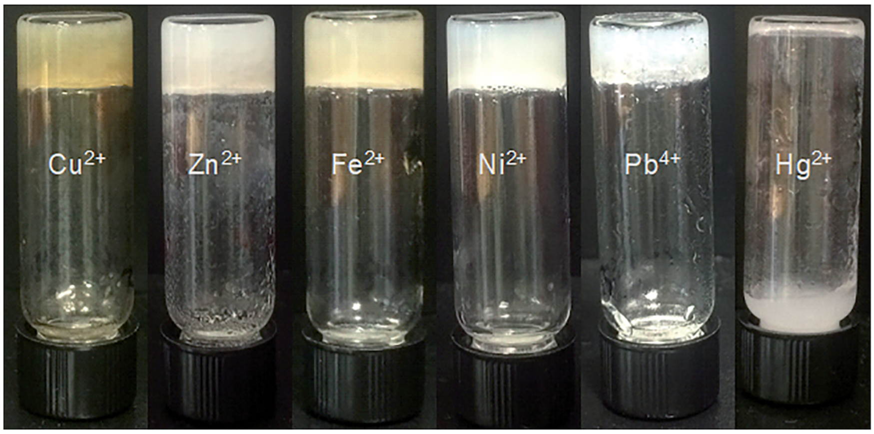

Fig. 3 Photograph of spontaneous gels containing Cu^{2+}, Zn^{2+}, Fe^{2+}, Ni^{2+}, Pb^{4+}. The mercury salt mixture only formed a precipitate. The solvent is DMSO : H_2O (v/v 1 : 1) and the molar ratio of gelator **18** to the metal ions is 1 : 2 for all samples.

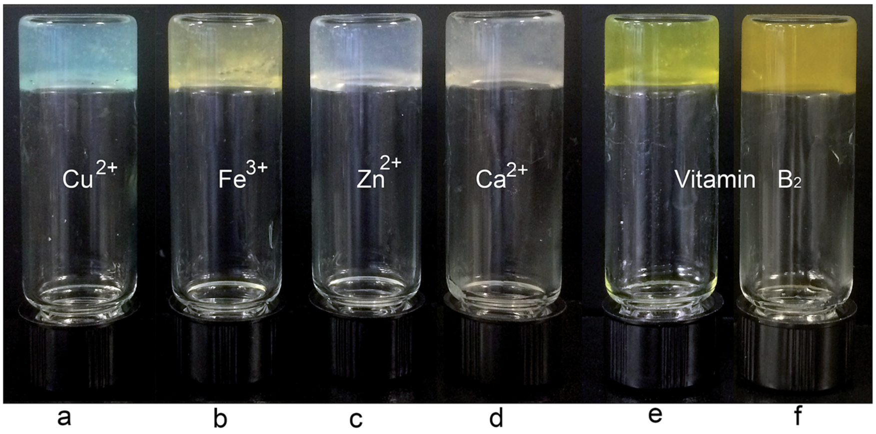

Fig. 4 Gels formed by compound **18** with different metal ions (a–d) and vitamin B_2 (e–f) in DMSO : H_2O (v/v 1 : 8). The molar ratio of gelator **18** to the metal ions are 1 : 5 for (a–d). The vitamin B_2 to gelator molar ratio was 1 : 19 in (e) and 1 : 2 in (f).

p-methoxyl benzyl carbamate **18** in EtOH : H_2O (v/v 1 : 1) showed bright birefringent fibers or tubular networks (Fig. 5a). The phenyl derivative **20** in DMSO : H_2O (v/v 1 : 1) formed smaller and shorter fibers (Fig. 5b). The gel of compound **18** in DMSO : H_2O (v/v 1 : 1) formed very long and uniform fibrous assemblies with smaller diameters (Fig. 5c). Compound **18** also formed gels in the presence of metal salts, the gel morphology showed some differences with the addition of various metals in comparison to the gel morphology without the metal salts. The Zn^{2+}-containing gel showed shorter but uniform fibrous networks (Fig. 5d), and the nickel ion containing gel apparently led to birefringent fibers with larger diameters and longer length than the zinc gel (Fig. 5e). Finally, in the presence of Fe^{2+}, the gels formed very long and straight fibers but less birefringent, and more densely packed fibrous assemblies (Fig. 5f). The optical micrograph also showed the fibers emerging and cross-linking within the solvent, forming the bulk of the gel. The presence of the metal ions seems to affect the molecular assembling process by forming extended uniform fibrous networks. The interaction of the compound **18** with metal ions led to enhanced intermolecular electrostatic interactions.

The SEM images for the dried gels of compounds **17** and **18** in EtOH : H_2O (v/v 1 : 1) are shown in Fig. 6. The benzyl derivative **17** formed very small and densely packed fibrous networks (Fig. 6a and b), however compound **18** formed wide planar sheet like assemblies (Fig. 6c and d), the individual sheets have an average diameter of 2.5 μm. Compound **17** had a relatively lower gelation concentration and it formed a smaller fibrous network with tiny fibers packing into more stacked smooth films. On the other hand, compound **18** had higher MGCs and it formed large planar sheets (Fig. 6d). The morphology of the dried gels has more local crystallinity order; a similar trend was observed from the optical micrographs (OMs) whereby the more efficient gelators typically formed smaller fibrous networks and the less efficient ones formed more rigid planar sheets or stacking ribbons.

The melting point ranges of some of the gels formed by hexyl carbamate **13**, heptyl carbamate **14**, and cyclohexyl carbamate **16** in 1 : 1 DMSO : H_2O were measured (Table 2). The three temperatures recorded were the temperature at which liquid was first seen, the temperature at which the gel was halfway melted, and the temperature at which the gel was fully melted to liquid. The gels started melting at 41.5–50.8 °C and completely melted at 77.2–122.2 °C. The melting point range for the gels increased as gel concentration decreased. All the gels measured in this experiment showed a large melting point range, which suggests that the gels are relatively stable to heat (Table 3).

The rheological properties of the gels formed by compounds **17** and **20** in several solvents were evaluated, these are shown in Fig. 7 and S5. For all gels, their storage moduli G' were greater than the loss moduli G'' in the full range of angular frequency from 0.1 to 100 rad S^{-1}, indicating the stability of the gels. The ethanol/water (1 : 2) gel of compound **17** had smaller G' and G'' compared to the gel of compound **20** in the same solvent. The gel formed by compound **20** in (EtOH : H_2O, 1 : 2) had the largest G' and G'' values among all the tested samples, and the toluene gel of compound **20** had the smallest G' and G'' values among all the tested samples.

NMR analysis at different temperatures to probe intermolecular forces

To analyze the structural impact on gelation, the ^{1}H NMR spectra at different temperatures for two representative compounds, the hexyl derivative **13** and phenyl derivative **20** were studied and these are shown in Fig. 8 and 9. Upon increasing temperatures from 30 to 60 °C in compound **13**, the NHAc chemical shift changed from 7.80 to 7.56 ppm, the amide proton shifted upfield by 0.24 ppm; and the carbamate NH signal also had an upfield change of 0.16 ppm. Compound **20** showed a similar upfield change for the two NH signals, the amide showed an upfield shift of 0.23 ppm and the carbamate moved upfield by 0.14 ppm. These indicate that both NH functional groups participated in the intermolecular hydrogen

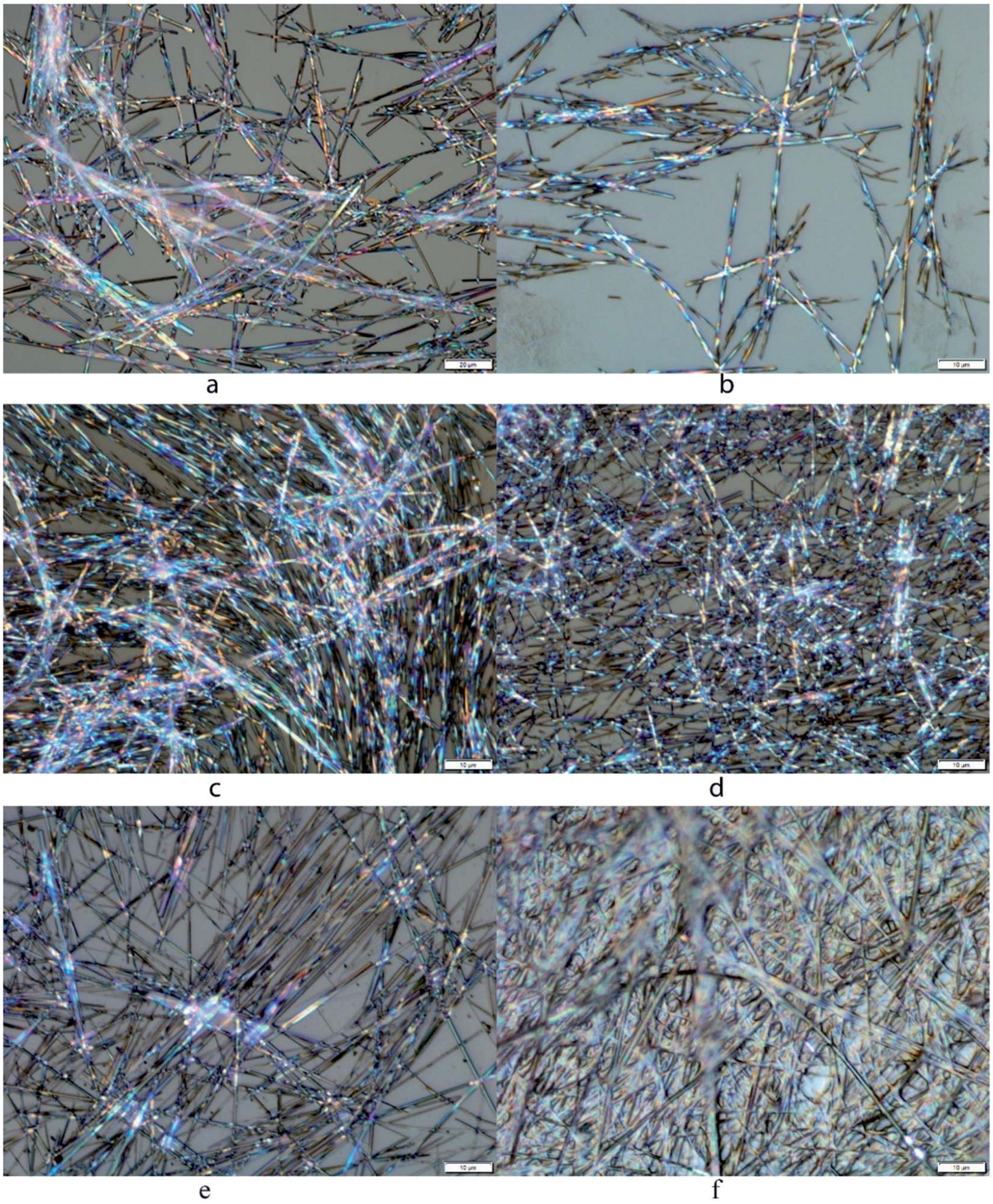

Fig. 5 Optical micrographs for several gels: (a) compound **18** in EtOH : H_2O (v/v 1 : 1) at 4.0 mg mL^{-1}, (b) compound **20** in DMSO : H_2O (v/v 1 : 1) at 4.0 mg mL^{-1}, (c) compound **18** in DMSO : H_2O (v/v 1 : 1) at 2.5 mg mL^{-1}, (d–f) compound **18** in DMSO : H_2O (v/v 1 : 1) and with added 2 equiv. of metal salts: (d) $Zn(OAc)_2$, (e) $Ni(OAc)_2$, (f) $FeCl_2$, the gelator concentration was 2.5 mg mL^{-1}, 5.1 mM.

bonding interactions. The acetamide showed a bigger shift which perhaps is due to less steric hindrance comparing to the carbamate at the C-3 position.

Naproxen entrapment and timed release studies

Due to the ease of syntheses of these carbamate derivatives, their applications for various other systems would be important. Compound **20** was utilized for the analysis of the encapsulation of naproxen as well as the transfer rate of the naproxen from the gel to the aqueous phase. This was monitored using UV-vis spectroscopy and the results are shown in Fig. 10. About 50% of the naproxen was released to the aqueous phase after 8 hours, and reached full equilibrium at about 2 days. The gels were stable during these measurements and no visible changes were noted. The gel photos are included in Fig. S15.†

Stability of the carbamates under basic conditions

These carbamates are interesting compounds that should be more stable in basic conditions in comparison to the

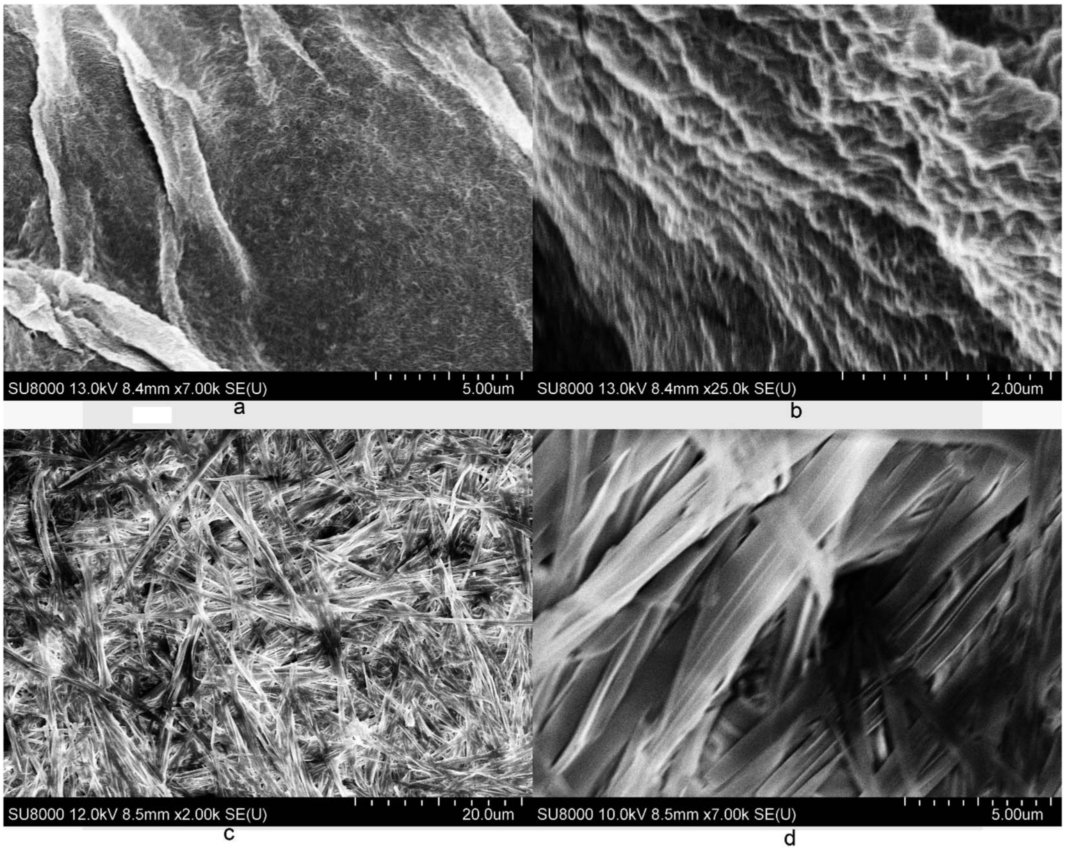

Fig. 6 Scanning electron micrographs for several gels: (a and b) compound **17** in EtOH : H_2O (v/v 1 : 1) at 2.5 mg mL^{-1}, (c and d) compound **18** in EtOH : H_2O (v/v 1 : 1) at 4.0 mg mL^{-1}.

Table 3 The melting point range for some of the gels in DMSO : H_2O (v/v 1 : 1)

Compound	Gelator conc. (mM)	mg mL^{-1}	T_1 (°C)	T_2 (°C)	T_3 (°C)
13	44.4	20.0	48.0	71.3	77.2
14	21.5	10.0	50.8	85.1	95.6
16	14.9	6.7	41.5	91.3	122.2

corresponding esters derivatives. The stability of several compounds in alkaline conditions was analyzed and the results are summarized in ESI Fig. S1.† The gels formed by the hexyl carbamate **13** and the benzyl derivative **17** in EtOH : H_2O (v/v 1 : 1) were chosen for the analysis. An equal volume of aqueous base (NaOH) at pH 10 or 12 solution was added on top of the gels. The stability of the gels in the presence of the basic solutions was observed by visual inspection and the gel stability was checked by tilting the vials at certain time intervals (14 h, 36 h, 144 h). All gels were stable at 14 h, the gels formed by **13** were stable in the presence of both basic solutions for 6 days, and the gel formed by **17** was stable in pH 10 solution for 6 days, but became unstable in pH 12 solution after 14 h. The mixture was analyzed after 6 days in pH 12 solution for compound **17**, the extracted compounds showed no decomposition under this condition (ESI Fig. S1 and S2†). Besides basic solutions, an organic base (DBU) was also used to analyze the stability of the *p*-methoxyl benzyl carbamate derivative **18**, the compound was dissolved in DMSO/H_2O (v/v 1 : 1), 5 equivalents of DBU was added to the solution, the mixture was heated and left standing at rt for 1 h, no decomposition was observed by TLC and ^1H NMR analysis (ESI Fig. S1–S3†). From this study, we showed that the carbamate gelators were resistant to base degradation, this property could be important with certain applications when the stability of gelators is required.

Gelation for electrolytes and response to anions or chemical stimuli

The carbamate derivative **18** also formed stable gels in the presence of tetramethylammonium bromide (TMABr) at 0.5, 5.0 and 10.0 equivalents. This indicates that the gelator can form stable co-gels with the ammonium salts, which are electrolytes.[42,52] The gelation response towards several tetrabutylammonium salts were also studied for compound **18**. In DMSO : H_2O (v/v 1 : 1) solvent, compound **18** formed stable gels with several tetrabutylammonium salts (TBAX). These include tetrabutylammonium salts of iodide, bromide, bisulfate, and fluoride; abbreviated as TBAI, TBABr, TBAHS, and TBAF. The initial TBAX amount (2.1 mM) was 0.5 equivalent to compound **18** (2.5 mg mL^{-1}, or 4.1 mM), stable gels were obtained for all four salts. To the same gels, addition of another 4.5 equivalents

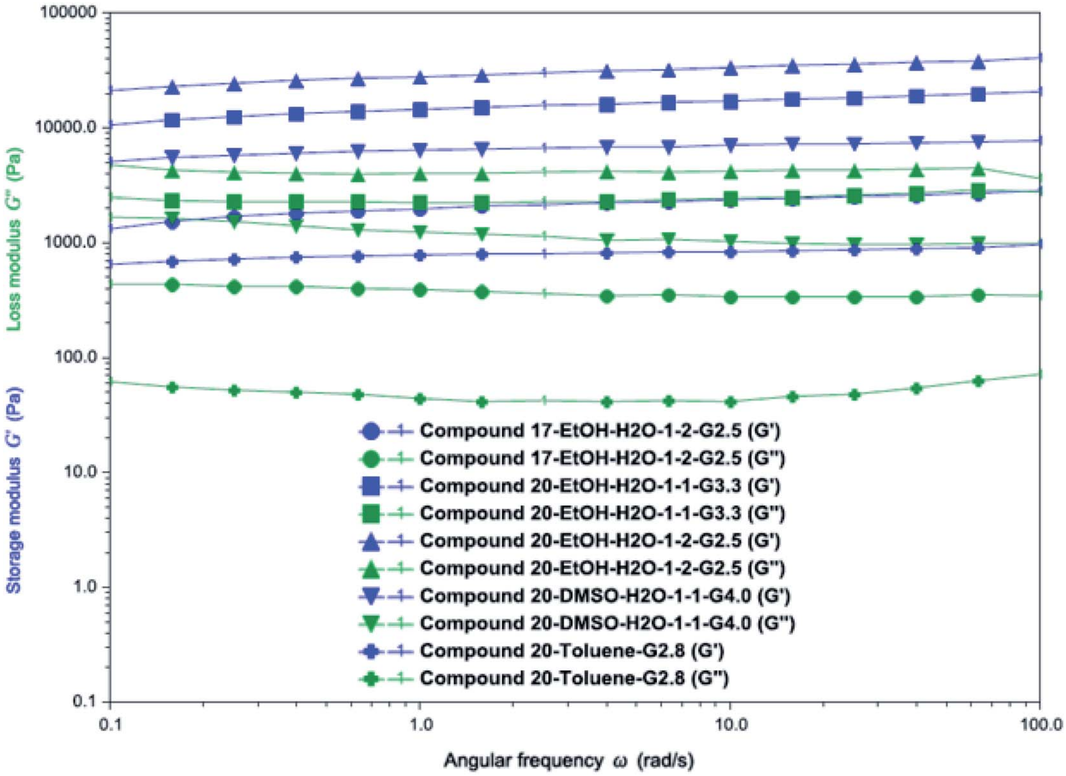

Fig. 7 Rheological properties of the gels formed by compound **17** (EtOH : H_2O, 1 : 2, 2.5 mg mL^{-1}), compound **20** (EtOH : H_2O, 1 : 1, 3.3 mg mL^{-1}), compound **20** (EtOH : H_2O, 1 : 2, 2.5 mg mL^{-1}), compound **20** (DMSO : H_2O, 1 : 1, 4.0 mg mL^{-1}) and compound **20** (toluene, 2.8 mg mL^{-1}). Applied strain was 1% for all the samples, all solvent ratios are volume ratios.

of TBA salts also resulted in stable gels as shown in Fig. S4a.† However upon further addition of another 5 equivalents of TBAX to the corresponding gels, the gels containing TBA salts of bromide and bisulfate became unstable, but the vials containing TBAI and TBAF were able to reform stable gels (Fig. S4b†). To the precipitated mixtures of the samples containing TBABr

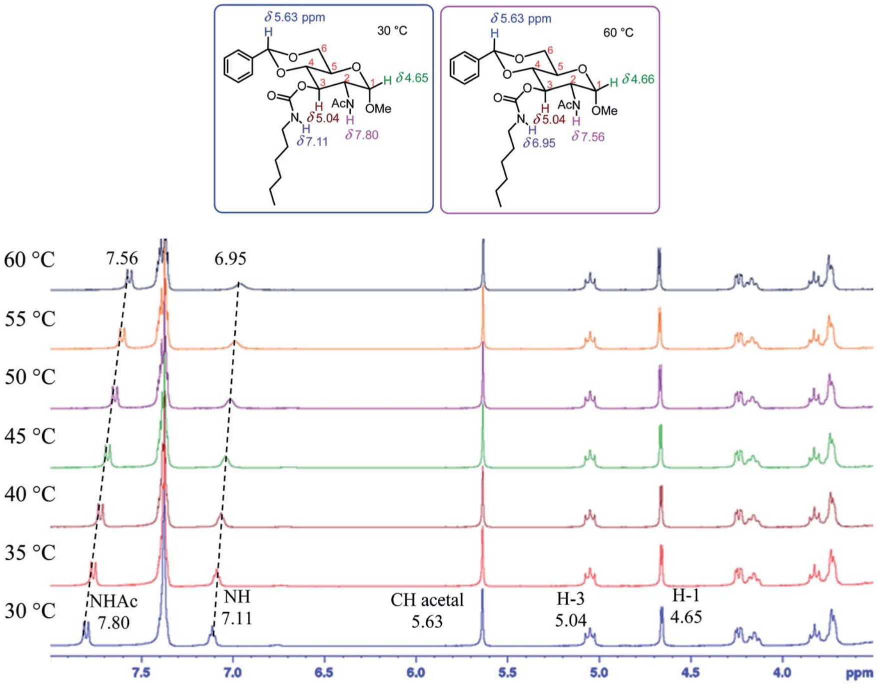

Fig. 8 The ^1H NMR spectra (3.5 to 8.0 ppm) of compound **13** from 30 °C to 60 °C in DMSO-d_6 (10.0 mg mL^{-1}).

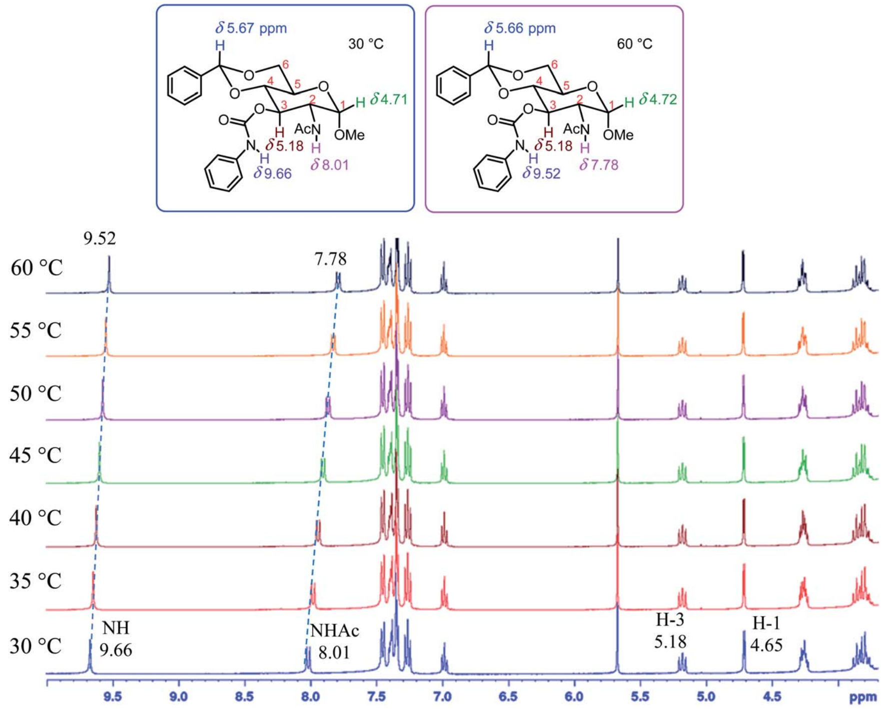

Fig. 9 The ^{1}H NMR spectra (3.7 to 10.0 ppm) of compound **20** from 30 °C to 60 °C in DMSO-d_6 (10.0 mg mL^{-1}).

and TBAHS, further addition of 10 equivalents of acetic acid led to the restoration of gels for TBABr, but not for TBAHS (Fig. S4c†). Fig. 11 shows the responses towards the salt and acid for samples with addition of TBABr salt.

NMR studies of gelators with different amounts of TBABr

The NMR spectra of gelator **18** with different amounts of TBABr were obtained in two different solvents, *d*-chloroform and d_6-acetone. Deuterated chloroform is a non-hydrogen bonding solvent and the interaction of gelator with the anions should be more pronounced. We observed a significant amount of chemical shift change for the gelator upon the addition of different amounts of the tetrabutylammonium salt (Fig. 12, S10 and S11†). However in d_6-acetone (Fig. S12†), not many chemical shift changes were observed with the added TBABr salt, which indicates that the gelator self-assembling mechanisms are very different in different solvents, the molecules will interact with the solvents significantly, therefore the effect of the ammonium salt was not important.

Compound **18** showed the greatest chemical shift changes in deuterated chloroform. The ^{1}H NMR spectra of gelator **18** with different amounts of TBABr are shown in Fig. 12. From 0 to 10 equivalents of TBABr, the NHAc chemical shift changed from 5.99 to 5.92 ppm, with an upfield shift of 0.07 ppm. Interestingly, the carbamate NH signal showed almost no change, and all other C–H signals moved about 0.1 ppm upfield. Consequently, with 15 equiv. of TBABr, nearly all C–H signals moved upfield by 0.14 ppm from 0 to 15 equivalents of the salt (Fig. S11†). This trend is the same for all hydrogens except the carbamate hydrogen NHCO, which stayed the same with more Br-ions and only showed 0.01 ppm upfield change from 5.09 to 5.08 ppm, this trend is very different compared to the rest of the compounds. The amide NHAc (δN–H) signal shifted upfield by 0.12 ppm, and most of other C–H signals showed an upfield chemical shift change of 0.14 ppm. The observed upfield change of δAr–H upon addition of more TBABr indicated that π–π stacking interactions of the aromatic functions are involved in the gelation process.[41,53,54] With increasing amount of TBABr, possible anion–π interaction is also present. On the other hand, other C–H signals moving upfield were probably due to CH–π interactions and enhanced van der Waals forces, these indicate that the sugar ring was also involved in gel formation. The NH signal of the carbamate participated in hydrogen bonding with the bromide, this effect does not change upon further addition of the salt, one equivalent of the salt was sufficient in forming the hydrogen bonds.

The same trend was observed for the aromatic carbamate **20**, in different solvents the chemical shift showed significantly different trends. In CDCl$_3$, with different amounts of TBABr from 0 to 10 equivalents, most of the C–H signals in compound **20** moved upfield by 0.10 ppm, with the C–H$_3$ displaying a 0.12 ppm change (Fig. 13 and S13†). The amide NHAc only showed a 0.06 ppm upfield shift from δ 6.01 to 5.95 ppm; and the carbamate NHb showed 0.06 ppm downfield change from δ 6.72 to 6.78 ppm, which is opposite to the others. This indicates that both the amide and carbamate NH participates in hydrogen bonding strongly and contributed to gelation. With the addition of more bromide ions, the C–H signals in the NMR spectra showed significant upfield changes, including both the aromatic peaks and the sugar ring C–H signals, which signified that at higher TBABr salt concentrations the gelator showed

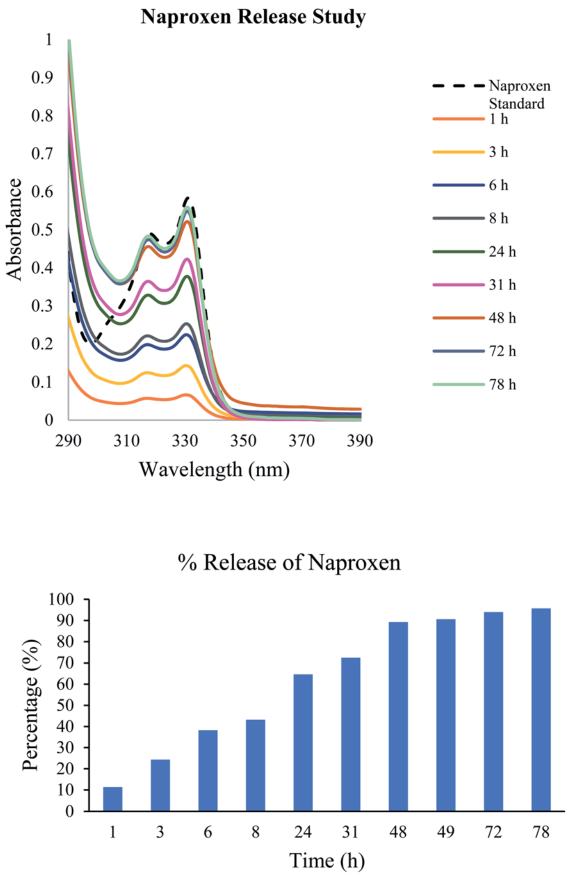

Fig. 10 Release of naproxen from the gel to the aqueous phase (a) UV spectra of naproxen release at different times from the gel formed by compound **20** (5.6 mg) in 2.0 mL of DMSO : H_2O (v/v 1 : 7) with naproxen (0.25 mg) in the presence of phosphate buffered saline at pH 7.47 (2.0 mL) on top of the gel. (b) The % release at different times based on the UV absorbance at 331 nm.

enhanced π–π stacking interactions and C–H–π interactions. In the DMSO solvent, the influence of the anion binding is much less than that of chloroform. In the DMSO-d_6 solvent (Fig. S14†) the signals did not show much change upon the titration of TBABr from 0 to 10 equivalents, the carbamate NHCO signal remained mostly unchanged (from 9.65 to 9.66 ppm), the NH signal showed slightly more upfield change of 0.05 ppm from δ 8.01 to 7.96 ppm. The acetal CH showed a small downfield change of 0.04 ppm from 5.66 to 5.70 ppm; whilst the C–H_3, and C–H_1 showed small upfield changes of 0.02 and 0.03 ppm, respectively.

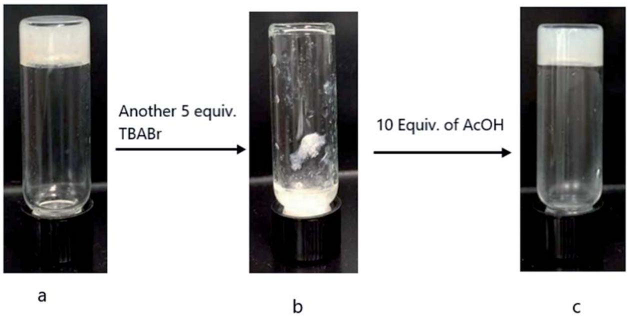

Fig. 11 Gelation properties of compound **18** with TBABr, (a) gel formed with 5 equiv. of TBABr, (b) precipitation with 10 equiv. of TBABr, (c) resumed gelation after adding acetic acid to the vial in (b).

Conclusions

A series of nineteen 3-*O*-carbamate derivatives of the *N*-acetyl-D-glucosamine headgroup has been synthesized and their self-assembling mechanisms in a variety of solvents were studied. The structure of the functional group attached to the carbamoyl moiety plays an important role in the gelation properties. The aliphatic carbamates were more effective than the aromatic derivatives with an exception of the phenyl carbamate. Interestingly, the dimeric sugar carbamate derivatives were not as effective gelators in comparison to the monomeric carbamate derivatives. Among these carbamate derivatives, most of the alkyl carbamates formed gels in pump oil and several also formed gels in mixed solvents of water with ethanol or water with DMSO. Certain aryl carbamates were also effective gelators for a few of the tested solvents. The best performing compounds are the *p*-methoxybenzyl derivative **18** and the phenyl carbamate **20** which formed gels in eight of the tested solvents and with low MGCs of up to 2.5 mg mL^{-1}. The compound **18** was also an effective gelator for metal ions and tetrabutylammonium salts. It formed spontaneous gels in the presence of several metal ions including Ca^{2+}, Cu^{2+}, Fe^{2+}, Zn^{2+}, and Ni^{2+}. Besides metal ions, the compound also formed stable gels in the presence of tetramethyl or tetrabutyl ammonium salts. The gels were characterized using optical microscopy, rheology and scanning electron microscopy. The gelators formed long and uniform fibrous networks as indicated by the optical micrographs and SEMs. The gelation properties of some representative compounds were further studied and analyzed using ^1H NMR spectroscopy at different temperatures and different amounts of the TBABr salts. The phenyl carbamate derivative was also used for entrapping and releasing naproxen. The structure and gelation properties obtained from this study will be used for the design of other relevant molecular gelators, these compounds will also be further studied for other applications such as sensors for bromide ions, *etc*.

Experimental section

General methods

Reagents and solvents were used as they were received from the suppliers. All purification was conducted by flash chromatography using 230–400 mesh silica gel obtained from Natland International Corporation. ^1H NMR and proton-decoupled ^{13}C NMR spectra were obtained with a Bruker 400 MHz spectrometer in DMSO-d_6 or $CDCl_3$. The chemical shifts were reported using $CDCl_3$/DMSO-d_6 as internal standard at 7.26/2.50 ppm and at 77.00/39.50 ppm, respectively. 2D NMR experiments (HSQC, COSY) were also conducted using a 400 MHz Bruker NMR spectrometer to assist the proton and carbon signal assignment. Melting point measurements were carried out

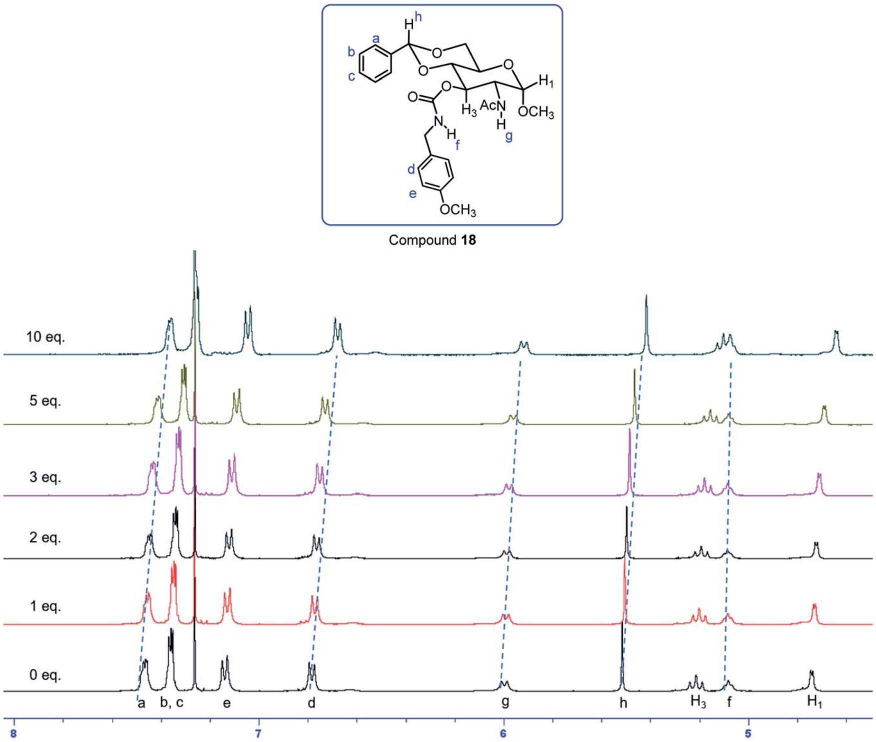

Fig. 12 ^{1}H NMR spectra of gelator **18** in $CDCl_3$ with different amount of tetrabutylammonium bromide (TBABr).

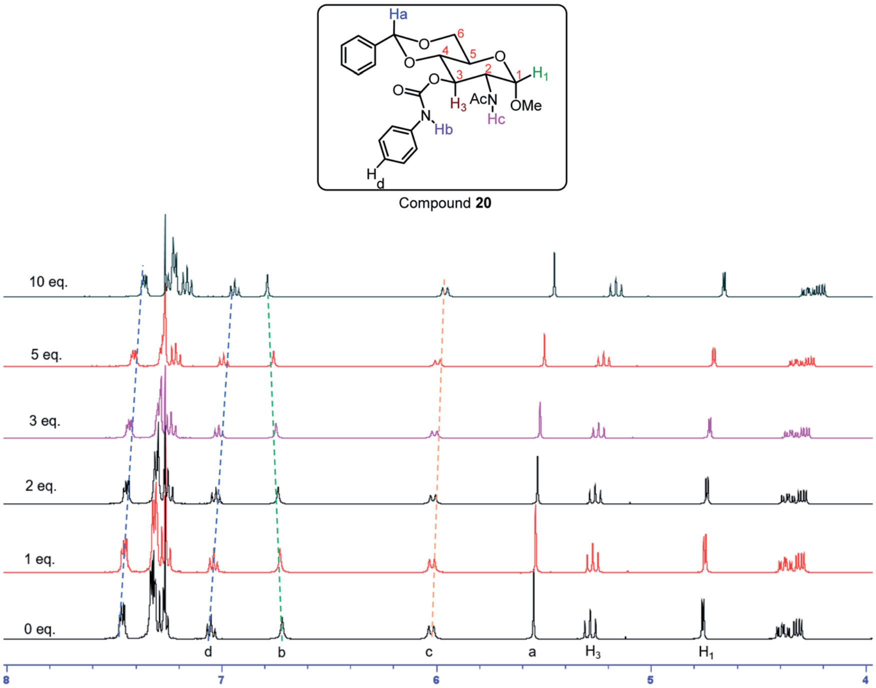

Fig. 13 ^{1}H NMR spectra of gelator **20** in $CDCl_3$ with different amount of tetrabutylammonium bromide (TBABr).

using a Fisher Jones melting point apparatus. The molecular mass was measured using LCMS on an Agilent 6120B Single Quad Mass Spectrometer and LC1260 system or Shimadzu LCMS-2020 with ESI in positive ionization mode.

Optical microscopy. A thin slice of the gel was transferred onto a clean glass slide and then left to air-dry for a day or so. The gel was then observed under an Olympus BX60M optical microscope using an Olympus DP73-1-51 high-performance

17MP digital camera with pixel shifting and Peltier cooling. The program used to acquire and store the images is CellSens Dimension 1.11.

Gelation test. Approximately 2 mg of the desired compound was placed in a one-dram vial and 0.1 mL of the gelation solvent or solution was transferred to the vial to attain a concentration of 20 mg mL^{-1}. The vial was then heated until the gelator dissolved fully; sometimes, the mixture was sonicated to help with dissolving the compound and the mixture was left to cool for approximately 15 minutes or longer for the gel to form. After this period, if the solution was clear, this was recorded as soluble; if the solid reappeared, this was recorded as a precipitate; if the sample formed a gel, then the vial was inverted; if no solvent was flowing, this indicated that a stable gel was formed; otherwise, this was recorded as an unstable gel. If gelation occurs, another 0.1 mL solvent is added and the method is repeated until an unstable gel is formed. The minimum gelation concentration (MGC) which represents the concentration prior to unstable gelation, was recorded.

For the gelation screening in DMSO and water mixtures, typically, about 2.0 mg of the compound was first dissolved in small amount of DMSO (0.1 mL), followed by addition of water (0.1 mL) incrementally until a stable gel can no longer form. The concentration of the stable gelation was recorded as the gelation concentration (Table 2).

Gelation test for metal ions. Compound **18** (2.0 mg, 4.11×10^{-3} mmol, 1 equivalent) was dissolved in 0.4 mL of DMSO in a 1 dram vial. Then the aqueous solution (2.05×10^{-2} mol L^{-1}) of $Cu(OAc)_2$, $Zn(OAc)_2 \cdot 2H_2O$, $FeCl_2$, $Ni(OAc)_2$, $Pb(OAc)_4$, $Hg(OAc)_2$, (0.4 mL, 8.22×10^{-3} mmol, 2.0 equivalents to compound **18**) was added to the vials. The samples were kept at room temperature for 20 min and the vials were inverted to examine if gelation occurred. The photos of the vials which exhibited spontaneous gels in 20 min are shown in Fig. 3.

Gelation tests in DMSO : H_2O (v/v 1 : 8). Compound **18** (2.0 mg, 4.11×10^{-3} mmol, 1 equivalent) was dissolved in 0.09 mL of DMSO in a 1 dram vial. Aqueous solutions (0.71 mL, 2.06×10^{-2} mol L^{-1}, 5 equivalent) of phosphocholine chloride calcium salt tetrahydrate, $Zn(OAc)_2 \cdot 2H_2O$, $Cu(OAc)_2 \cdot H_2O$ and $FeCl_3$ were added to the above DMSO solution at room temperature, respectively. For the vitamin B_2 gelation test, compound **18** (2.0 mg, 4.11×10^{-3} mmol, 1 equivalent) was dissolved in 0.09 mL of DMSO in a 1 dram vial, then an aqueous solution (0.71 mL, 2.99×10^{-4} mol L^{-1} and 2.48×10^{-3} mol L^{-1}) of riboflavin B_2 was added to the above DMSO solution at room temperature, respectively. The gel photos are shown in Fig. 4.

Scanning electron microscopy (SEM). A thin slice of the gel was transferred on to a clean glass slide (1.0 mm × 1.0 mm) and then left to air-dry for at least one day, afterwards it was placed in a desiccator for additional two days. The sample was then coated with a thin layer of gold (~50 nm) using a sputter coater (BOC Edwards 306 Evaporator, <10^{-6} torr). The sample was observed, and images were taken using SU8010 Hitachi field emission scanning electron microscope.

Naproxen trapping and release studies. Naproxen sodium was dissolved in the desired solvent, and this was used to prepare the gel first. Naproxen sodium (2.5 mg) was dissolved in 10.0 mL of DMSO : H_2O (v/v 1 : 7). This solution (2 mL) was used to prepare the gel with compound **20** (5.6 mg). The gelator concentration was 2.8 mg mL^{-1}, and the initial naproxen sodium concentration was 0.25 mg mL^{-1}. The gel was left at room temperature for 14 hours, and then phosphate buffered saline (pH 7.47) was placed on top of the gel. The UV absorbance of the aqueous phase was taken at different time intervals by transferring the solution to a cuvette and then cautiously returning it to the vial after the measurement. The final naproxen concentration should be 0.125 mg mL^{-1} in both aqueous and gel phases if equilibrium has been achieved. Phosphate buffered saline was made by dissolving 8.01 of sodium chloride, 0.2 g of potassium chloride, 2.72 g of di-sodium hydrogen phosphate heptahydrate and 0.27 g of potassium dihydrogen phosphate in 1.0 L of DI water. This was autoclaved for 20 minutes at 121 °C or filtered using a 0.45 μm filter to sterilize.

Synthesis of carbamate derivatives

Compounds **12–14**, **16**, **17**, **20–23** were prepared using the methods described previously.[51] The other compounds **9–11**, **15**, **18–19**, **24–27** were synthesized using the CDI method. The detailed procedures are given for one mono-carbamate and one di-carbamate. Only the characterization data of other compounds were given unless the method used was different.

Synthesis of imidazole carboxylate compound 8. Compound **7** (1.00 g, 3.13 mmol, 1 equiv.) and CDI (1.02 g, 6.26 mmol, 2 equiv.) were dissolved in anhydrous DCM (10 mL). The reaction mixture was stirred at room temperature for 2 hours under N_2 at which ^1H NMR spectrum showed full conversion. The mixture was washed with water (2 mL × 2) and the combined organic phases were dried over Na_2SO_4. The solvent was removed to give the crude, which was purified by column chromatography using eluent from 0.5% to 5% MeOH/DCM to afford a white solid (1.25 g, 2.99 mmol, 96%) as the desired product. $R_f = 0.3$ in 2% MeOH/DCM; mp 245.0–246.0 °C. ^1H NMR (400 MHz, $CDCl_3$) δ 8.12 (s, 1H), 7.42–7.40 (m, 3H), 7.34–7.31 (m, 3H), 7.04 (s, 1H), 5.94 (d, $J = 9.8$ Hz, 1H), 5.54 (s, 1H), 5.39 (t, $J = 9.9$ Hz, 1H), 4.76 (d, $J = 3.7$ Hz, 1H), 4.58 (dt, $J = 10.2$, 3.7 Hz, 1H), 4.33 (dd, $J = 10.2$, 4.7 Hz, 1H), 3.97–3.91 (m, 1H), 3.89–3.80 (m, 2H), 3.44 (s, 3H), 1.91 (s, 3H); ^{13}C NMR (100 MHz, $CDCl_3$) δ 170.0, 148.8, 137.3, 136.6, 130.8, 129.2, 128.2, 126.1, 117.3, 101.7, 99.0, 78.8, 75.0, 68.8, 62.8, 55.4, 51.8, 23.1. LC-MS (ESI+) calcd for $C_{20}H_{24}N_3O_7$ $[M + H]^+$ 418.2, found 418.2.

General procedure for carbamate synthesis using CDI method

For mono-carbamate synthesis, the imidazole carboxylate **8** (75 mg, 0.18 mmol, 1.0 equiv.), amine (1.2 or 1.5 equiv.) and 2 mL of anhydrous DCM were added to a 50 mL round bottomed flask. For bis-carbamate synthesis, compound **8** (120 mg, 0.29 mmol, 2.1 equiv.), di-amine (1.0 equiv.) and 2 mL of anhydrous DCM were added to a 50 mL round bottom flask. The mixture was stirred at room temperature until full conversion was confirmed by ^{1}H NMR analysis. The solvent was removed to give the crude product, which was further purified by column chromatography using eluent from 0.5% MeOH/DCM to 5% MeOH/DCM to afford the purified carbamate derivatives.

Synthesis of compound 9. Compound **8** (100 mg, 0.24 mmol, 1.0 equiv.) and propargylamine (0.023 mL, 0.36 mmol, 1.5 equiv.) were added to a 50 mL round bottom flask. The mixture was stirred for 8 hours at room temperature. A white solid (81 mg, 84%) was obtained as the desired product (R_f = 0.5 in 5% MeOH/DCM). mp 220.1–223.0 °C; ^{1}H NMR (400 MHz, $CDCl_3$) δ 7.49–7.43 (m, 2H), 7.37–7.31 (m, 3H), 6.00 (d, J = 9.3 Hz, 1H), 5.52 (s, 1H), 5.19 (t, J = 10.0 Hz, 1H), 5.04 (br s, 1H), 4.73 (d, J = 3.4 Hz, 1H), 4.36–4.25 (m, 2H), 4.02–3.81 (m, 3H), 3.79 (t, J = 10.2 Hz, 1H), 3.68 (t, J = 9.5 Hz, 1H), 3.40 (s, 3H), 2.18 (br s, 1H), 1.98 (s, 3H); ^{13}C NMR (100 MHz, $CDCl_3$) δ 169.3, 155.0, 136.0, 128.1, 127.2, 125.3, 100.7, 98.1, 78.4, 78.2, 70.6, 70.3, 67.9, 61.9, 54.3, 51.9, 29.8, 22.3. LC-MS (ESI+) calcd for $C_{20}H_{25}N_2O_7$ $[M + H]^+$ 405, found 405.

Synthesis of compound 10. Compound **8** (75 mg, 0.18 mmol, 1.0 equiv.) and 3-butynylamine (0.022 mL, 0.27 mmol, 1.5 equiv.) were added to a 50 mL round bottom flask. The mixture was stirred for 5 hours at room temperature. A white solid (65 mg, 87%) was obtained as the desired product (R_f = 0.36 in 5% MeOH/DCM). mp 192.0–194.2 °C; ^{1}H NMR (400 MHz, $CDCl_3$) δ 7.50–7.43 (m, 2H), 7.38–7.31 (m, 3H), 6.03 (d, J = 8.9 Hz, 1H), 5.52 (s, 1H), 5.24–5.09 (m, 2H), 4.74 (d, J = 3.5 Hz, 1H), 4.34–4.23 (m, 2H), 3.92–3.84 (m, 1H), 3.82–3.73 (m, 1H), 3.67 (t, J = 9.4 Hz, 1H), 3.40 (s, 3H), 3.32–3.24 (m, 2H), 2.38–2.32 (m, 2H), 1.97 (s, 3H), 1.96 (t, J = 2.6 Hz, 1H); ^{13}C NMR (100 MHz, $CDCl_3$) δ 170.2, 156.4, 137.1, 129.1, 128.2, 126.3, 101.6, 99.1, 81.0, 79.3, 70.9, 70.2, 68.9, 62.9, 55.3, 53.0, 39.8, 23.2, 19.6. LC-MS (ESI+) calcd for $C_{21}H_{27}N_2O_7$ $[M + H]^+$ 419, found 419.

Synthesis of compound 11. Compound **8** (75 mg, 0.18 mmol, 1.0 equiv.) and 1-butylamine (0.027 mL, 0.27 mmol, 1.5 equiv.) were added. The mixture was stirred for 11 hours at room temperature. A white solid (65 mg, 86%) was obtained as the desired product (R_f = 0.42 in 5% MeOH/DCM). mp 209.0–211.1 °C; ^{1}H NMR (400 MHz, $CDCl_3$) δ 7.47–7.44 (m, 2H), 7.36–7.33 (m, 3H), 6.07 (d, J = 9.1 Hz, 1H), 5.52 (s, 1H), 5.17 (t, J = 10.1 Hz, 1H), 4.78 (t, J = 5.4 Hz, 1H), 4.74 (d, J = 3.3 Hz, 1H), 4.30–4.23 (m, 2H), 3.91–3.84 (m, 1H), 3.78 (t, J = 10.1 Hz, 1H), 3.66 (t, J = 9.5 Hz, 1H), 3.39 (s, 3H), 3.20–3.07 (m, 2H), 1.97 (s, 3H), 1.46–1.39 (m, 2H), 1.34–1.26 (m, 2H), 0.88 (t, J = 7.1 Hz, 3H); ^{13}C NMR (100 MHz, $CDCl_3$) δ 170.2, 156.5, 137.1, 129.1, 128.2, 126.3, 101.6, 99.1, 79.3, 70.6, 69.0, 62.9, 55.3, 53.2, 40.8, 31.9, 23.2, 19.8, 13.7. LC-MS (ESI+) calcd for $C_{21}H_{31}N_2O_7$ $[M + H]^+$ 423, found 423.

Synthesis of compound 16. Compound **8** (100 mg, 0.24 mmol, 1.0 equiv.) and cyclohexylamine (35.7 mg, 0.36 mmol, 1.5 equiv.) were added to a 50 mL round bottom flask. The mixture was stirred for 12 hours at room temperature. A white solid (78 mg, 89%) was obtained as the desired product (R_f = 0.3 in 5% MeOH/DCM). The characterization data are the same as reported previously.[51]

Synthesis of compound 18. Compound **8** (100 mg, 0.24 mmol, 1 equiv.) and 4-methoxybenzylamine (0.037 mL, 0.29 mmol, 1.2 equiv.) were added to a 50 mL round bottom flask. The mixture was stirred for 4 hours at room temperature. A white solid (105 mg, 90%) was obtained as the desired product (R_f = 0.3 in 2% MeOH/DCM); mp 251.0–252.5 °C; ^{1}H NMR (400 MHz, $CDCl_3$) δ 7.47–7.45 (m, 2H), 7.36–7.35 (m, 3H), 7.13 (d, J = 8.4 Hz, 2H), 6.78 (d, J = 8.4 Hz, 2H), 6.03 (d, J = 9.0 Hz, 1H), 5.51 (s, 1H), 5.21 (t, J = 10.0 Hz, 1H), 5.11 (t, J = 5.7 Hz, 1H), 4.74 (d, J = 3.4 Hz, 1H), 4.30–4.23 (m, 4H), 3.91–3.85 (m, 1H), 3.82–3.72 (m, 4H), 3.66 (t, J = 9.4 Hz, 1H), 3.40 (s, 3H), 1.90 (s, 3H); ^{13}C NMR (100 MHz, $CDCl_3$) δ 170.3, 159.0, 156.5, 137.1, 130.3, 129.1, 128.6, 128.2, 126.3, 114.0, 101.7, 99.1, 79.3, 70.9, 69.0, 62.9, 55.3, 53.0, 44.5, 23.2. LC-MS (ESI+) calcd for $C_{25}H_{31}N_2O_8$ $[M + H]^+$ 487.2, found 487.2.

Synthesis of compound 19. Compound **8** (75 mg, 0.18 mmol, 1.0 equiv.) and 4-aminobenzylamine (0.031 mL, 0.27 mmol, 1.5 equiv.) were added to a 50 mL round bottom flask. The mixture was stirred for 12 hours at room temperature. A white solid (66 mg, 78%) was obtained as the desired product (R_f = 0.35 in 5% MeOH/DCM). mp 208.1–210.0 °C; ^{1}H NMR (400 MHz, $CDCl_3$) δ 7.51–7.43 (m, 2H), 7.40–7.31 (m, 3H), 7.00 (d, J = 7.9 Hz, 2H), 6.56 (d, J = 7.9 Hz, 2H), 6.07 (d, J = 8.9 Hz, 1H), 5.51 (s, 1H), 5.21 (t, J = 10.1 Hz, 1H), 5.07 (br s, 1H), 4.73 (d, J = 2.7 Hz, 1H), 4.33–4.11 (m, 4H), 3.93–3.84 (m, 1H), 3.79 (t, J = 10.2 Hz, 1H), 3.70–3.54 (m, 3H), 3.39 (s, 3H), 1.91 (s, 3H); ^{13}C NMR (100 MHz, $CDCl_3$) δ 170.3, 156.5, 145.8, 137.1, 129.1, 128.7, 128.2, 128.0, 126.3, 115.2, 101.7, 99.1, 79.3, 70.8, 69.0, 62.9, 55.3 (2 OCH_3), 53.1, 44.7, 23.2. LC-MS (ESI+) calcd for $C_{24}H_{30}N_3O_7$ $[M + H]^+$ 472, found 472.

Synthesis of compound 24. Compound **8** (120 mg, 0.288 mmol, 2.1 equiv.), *m*-xylylene diamine (18.6 mg, 0.137 mmol, 1.0 equiv.) were added to a 50 mL round bottom flask. The mixture was stirred for 6 hours at room temperature. A white solid (91 mg, 80%) was obtained as the desired product. R_f = 0.3 in 5% MeOH/DCM. mp > 275.0 °C; ^{1}H NMR (400 MHz, DMSO-d_6) δ 7.84 (d, J = 9.4 Hz, 2H), 7.68 (t, J = 6.1 Hz, 2H), 7.40–7.35 (m, 10H), 7.00–6.93 (m, 4H), 5.65 (s, 2H), 5.10 (t, J = 9.8 Hz, 2H), 4.66 (d, J = 3.5 Hz, 2H), 4.25–3.97 (m, 8H), 3.84–3.72 (m, 6H), 3.36 (s, 6H), 1.77 (s, 6H); ^{13}C NMR (100 MHz, DMSO-d_6) δ 170.1, 156.6, 140.1, 137.9, 129.3, 128.6, 128.5, 126.6, 125.8, 125.3, 101.0, 99.5, 79.8, 69.9, 68.4, 63.2, 55.5, 52.3, 44.0, 22.8. LC-MS (ESI+) calcd for $C_{42}H_{51}N_4O_{14}$ $[M + H]^+$ 835.3, found 835.3.

Synthesis of compound 25. Compound **8** (120 mg, 0.288 mmol, 2.1 equiv.) and ethylenediamine (8.2 mg, 0.137 mmol, 1 equiv.) were added to a 50 mL round bottom flask. The mixture was stirred for 4 hours at room temperature. A white solid (76.8 mg, 74%) was obtained as the desired product. R_f = 0.3 in 5% MeOH/DCM. mp > 275.0 °C; ^{1}H NMR (400 MHz, $CDCl_3$ + d_4-MeOH) δ 7.38–7.37 (m, 4H), 7.28–7.26 (m, 6H), 6.71 (d, J = 9.5 Hz, 2H), 5.42 (s, 2H), 5.03 (t, J = 9.9 Hz, 2H), 4.64 (d, J = 3.5 Hz, 2H), 4.23–4.16 (m, 4H), 3.84–3.78 (m, 2H), 3.71 (t, J = 10.2 Hz, 2H), 3.60 (t, J = 9.5 Hz, 2H), 3.35 (s, 6H), 3.19–3.08 (m, 4H), 1.85 (s, 6H); ^{13}C NMR (100 MHz, $CDCl_3$ + d_4-MeOH) δ 171.5, 156.9, 136.9, 129.1, 128.2, 126.2, 101.7, 99.0, 79.2, 70.9, 68.8, 62.7, 55.3, 52.7, 40.7, 22.7. LC-MS (ESI+) calcd for $C_{36}H_{47}N_4O_{14}$ $[M + H]^+$ 759.3, found 759.3.

Synthesis of compound 26. Compound **8** (120 mg, 0.288 mmol, 2.1 equiv.), 1, 3-diaminopropane (10.1 mg, 0.137 mmol, 1 equiv.) were added to a 50 mL round bottom flask. The mixture was stirred for 6 hours at room temperature. A white solid (77 mg, 73%) was obtained as the desired product. $R_f = 0.3$ in 5% MeOH/DCM. mp > 275.0 °C; ^{1}H NMR (400 MHz, $CDCl_3$) δ 7.44–7.43 (m, 4H), 7.31–7.29 (m, 6H), 6.09 (d, J = 8.9 Hz, 2H), 5.52 (s, 2H), 5.20–5.12 (m, 4H), 4.74 (d, J = 3.6 Hz, 2H), 4.32–4.27 (m, 4H), 3.91–3.85 (m, 2H), 3.79 (t, J = 10.2 Hz, 2H), 3.67 (t, J = 9.5 Hz, 2H), 3.41 (s, 6H), 3.05 (m, 4H), 1.95 (s, 6H); 1.56–1.47 (m, 2H); ^{13}C NMR (100 MHz, $CDCl_3$) δ 170.2, 156.9, 137.0, 129.1, 128.2, 126.3, 101.7, 99.1, 79.4, 70.9, 68.9, 62.9, 55.4, 52.8, 37.3, 29.8, 23.2. LC-MS (ESI+) calcd for $C_{37}H_{49}N_4O_{14}$ $[M + H]^+$ 773.3, found 773.3.

Synthesis of compound 27. Compound **8** (120 mg, 0.288 mmol, 2.1 equiv.), 1,6-hexanediamine (15.9 mg, 0.137 mmol, 1 equiv.) were added to a 50 mL round bottom flask. The mixture was stirred for 12 hours at room temperature. A white solid (90.3 mg, 0.11 mmol, 81%) was obtained as the desired product ($R_f = 0.4$ in 5% MeOH/DCM). mp > 275.0 °C; ^{1}H NMR (400 MHz, $CDCl_3$ + d_4-MeOH) δ 7.47–7.40 (m, 4H), 7.35–7.28 (m, 6H), 6.28 (d, J = 8.8 Hz, 2H), 5.53 (s, 2H), 5.19 (t, J = 10.1 Hz, 2H), 4.89–4.81 (m, 2H), 4.76 (d, J = 3.4 Hz, 2H), 4.37–4.25 (m, 4H), 3.96–3.86 (m, 2H), 3.81 (t, J = 10.2 Hz, 2H), 3.71 (t, J = 9.6 Hz, 2H), 3.42 (s, 6H), 3.02–2.81 (m, 4H), 1.97 (s, 6H), 1.39–1.28 (m, 4H), 1.23–1.16 (m, 4H); ^{13}C NMR (100 MHz, $CDCl_3$ + d_4-MeOH) δ 171.1, 156.7, 137.0, 129.0, 128.1, 126.2, 101.6, 99.1, 79.5, 70.3, 68.8, 62.8, 55.3, 52.7, 40.3, 29.1, 25.7, 22.8. LC-MS (ESI+) calcd for $C_{40}H_{55}N_4O_{14}$ $[M + H]^+$ 815.4, found 815.4.

Conflicts of interest

There are no conflicts to declare.

Acknowledgements

We are grateful for financial support from the National Science Foundation grant CHE# 1808609. We thank Dr Lalith Samankumara and Ms. Consuelo Garcia for their assistance with synthesis and analysis of some compounds. We also thank Dr Harold O. Lee III for his assistance with using scanning electron microscope.

References

1 D. Yuan and B. Xu, *J. Mater. Chem. B*, 2016, **4**, 5638–5649.

2 M. D. Segarra-Maset, V. J. Nebot, J. F. Miravet and B. Escuder, *Chem. Soc. Rev.*, 2013, **42**, 7086–7098.

3 A. H. Karoyo and L. D. Wilson, *Gels*, 2017, **3**, 1.

4 M. Liu, G. Ouyang, D. Niu and Y. Sang, *Org. Chem. Front.*, 2018, **5**, 2885–2900.

5 X. Du, J. Zhou, J. Shi and B. Xu, *Chem. Rev.*, 2015, **115**, 13165–13307.

6 L. A. Estroff and A. D. Hamilton, *Chem. Rev.*, 2004, **104**, 1201–1217.

7 A. Tanaka, Y. Fukuoka, Y. Morimoto, T. Honjo, D. Koda, M. Goto and T. Maruyama, *J. Am. Chem. Soc.*, 2015, **137**, 770–775.

8 J. Zeng, Y. Yin, L. Zhang, W. Hu, C. Zhang and W. Chen, *Macromol. Biosci.*, 2016, **16**, 363–370.

9 K. Lalitha, Y. S. Prasad, C. U. Maheswari, V. Sridharan, G. John and S. Nagarajan, *J. Mater. Chem. B*, 2015, **3**, 5560–5568.

10 B. Escuder, F. Rodriguez-Llansola and J. F. Miravet, *New J. Chem.*, 2010, **34**, 1044–1054.

11 B. O. Okesola and D. K. Smith, *Chem. Soc. Rev.*, 2016, **45**, 4226–4251.

12 H. Oh, N. Yaraghi and S. R. Raghavan, *Langmuir*, 2015, **31**, 5259–5264.

13 R. Balamurugan, Y. S. Zhang, S. Fitriyani and J. H. Liu, *Soft Matter*, 2016, **12**, 5214–5223.

14 M. Piccinno, C. A. Angulo-Pachon, P. Ballester, B. Escuder and A. D. Cort, *RSC Adv.*, 2016, **6**, 57306–57309.

15 P. Byrne, G. O. Lloyd, L. Applegarth, K. M. Anderson, N. Clarke and J. W. Steed, *New J. Chem.*, 2010, **34**, 2261–2274.

16 L. Viau, C. Tourne-Peteilh, J.-M. Devoisselle and A. Vioux, *Chem. Commun.*, 2010, **46**, 228–230.

17 T. Xiao and L. Wang, *Tetrahedron Lett.*, 2018, **59**, 1172–1182.

18 T. Xiao, L. Xu, L. Zhou, X.-Q. Sun, C. Lin and L. Wang, *J. Mater. Chem. B*, 2019, **7**, 1526–1540.

19 H. Maeda, *Chem.–Eur. J.*, 2008, **14**, 11274–11282.

20 H. Wu, J. Zheng, A. L. Kjoniksen, W. Wang, Y. Zhang and J. Ma, *Adv. Mater.*, 2019, **31**, e1806204.

21 M. O. Piepenbrock, G. O. Lloyd, N. Clarke and J. W. Steed, *Chem. Rev.*, 2010, **110**, 1960–2004.

22 J. Le Bideau, L. Viau and A. Vioux, *Chem. Soc. Rev.*, 2011, **40**, 907–925.

23 A. Ghosh, P. Das, R. Kaushik, K. K. Damodaran and D. A. Jose, *RSC Adv.*, 2016, **6**, 83303–83311.

24 N. Malviya, M. Das, P. Mandal and S. Mukhopadhyay, *Soft Matter*, 2017, **13**, 6243–6249.

25 Y. Zhai, W. Chai, W. Cao, Z. Sun and Y. Huang, *Front. Chem. Sci. Eng.*, 2015, **9**, 488–493.

26 Q. Lin, X. Zhu, Y.-P. Fu, Y.-M. Zhang, R. Fang, L.-Z. Yang and T.-B. Wei, *Soft Matter*, 2014, **10**, 5715–5723.

27 N. Malviya, C. Sonkar, B. K. Kundu and S. Mukhopadhyay, *Langmuir*, 2018, **34**, 11575–11585.

28 P. Xue, B. Yao, P. Wang, P. Gong, Z. Zhang and R. Lu, *Chem.–Eur. J.*, 2015, **21**, 17508–17515.

29 S. Sarkar, S. Dutta, S. Chakrabarti, P. Bairi and T. Pal, *ACS Appl. Mater. Interfaces*, 2014, **6**, 6308–6316.

30 L. Li, N. Zhou, H. Kong and X. He, *Polym. Chem.*, 2019, **10**, 5465–5472.

31 H. Yao, J. Wang, Q. Zhou, X.-W. Guan, Y.-Q. Fan, Y.-M. Zhang, T.-B. Wei and Q. Lin, *Soft Matter*, 2018, **14**, 8390–8394.

32 L. He, Z. W. Peng, Z. W. Jiang, X. Q. Tang, C. Z. Huang and Y. F. Li, *ACS Appl. Mater. Interfaces*, 2017, **9**, 31834–31840.

33 J. Zhou, J. Li, X. Du and B. Xu, *Biomaterials*, 2017, **129**, 1–27.

34 S. S. Babu, V. K. Praveen and A. Ajayaghosh, *Chem. Rev.*, 2014, **114**, 1973–2129.

35 F. Ono, H. Watanabe and S. Shinkai, *RSC Adv.*, 2014, **4**, 25940–25947.

36 S. Datta and S. Bhattacharya, *Chem. Soc. Rev.*, 2015, **44**, 5596–5637.

37 J. G. Hardy, A. R. Hirst, I. Ashworth, C. Brennan and D. K. Smith, *Tetrahedron*, 2007, **63**, 7397–7406.
38 O. Demir-Ordu, H. Simsir and K. Alper, *Tetrahedron*, 2015, **71**, 1529–1539.
39 G. Wang, S. Cheuk, K. Williams, V. Sharma, L. Dakessian and Z. Thorton, *Carbohydr. Res.*, 2006, **341**, 705–716.
40 G. Wang, S. Cheuk, H. Yang, N. Goyal, P. V. N. Reddy and B. Hopkinson, *Langmuir*, 2009, **25**, 8696–8705.
41 J. E. Webb, M. J. Crossley, P. Turner and P. Thordarson, *J. Am. Chem. Soc.*, 2007, **129**, 7155–7162.
42 M. Bielejewski, K. Nowicka, N. Bielejewska and J. Tritt-Goc, *J. Electrochem. Soc.*, 2016, **163**, G187–G195.
43 C.-C. Tsai, W.-T. Chuang, Y.-F. Tsai, J.-T. Li, Y.-F. Wu and C.-C. Liao, *J. Mater. Chem. B*, 2013, **1**, 819–827.
44 S. Baddi, D. S. Sarma and A. Palanisamy, *J. Sol-Gel Sci. Technol.*, 2016, **79**, 637–649.
45 L. Lascialfari, G. Pescitelli, A. Brandi, M. Mannini, D. Berti and S. Cicchi, *Soft Matter*, 2015, **11**, 8333–8341.
46 A. D'Aleo, J.-L. Pozzo, K. Heuze, F. Voegtle and F. Fages, *Tetrahedron*, 2007, **63**, 7482–7488.
47 A. Chen, L. P. Samankumara, C. Garcia, K. Bashaw and G. Wang, *New J. Chem.*, 2019, **43**, 7950–7961.
48 G. Wang, N. Goyal, H. P. R. Mangunuru, H. Yang, S. Cheuk and P. V. N. Reddy, *J. Org. Chem.*, 2015, **80**, 733–743.
49 N. Goyal, S. Cheuk and G. Wang, *Tetrahedron*, 2010, **66**, 5962–5971.
50 G. Wang, A. Chen, H. P. R. Mangunuru and J. R. Yerabolu, *RSC Adv.*, 2017, **7**, 40887–40895.
51 A. Chen, D. Wang, L. P. Samankumara and G. Wang, *Synthesis*, 2019, **51**, 2897–2908.
52 M. Bielejewski, A. Lapinski and O. Demchuk, *J. Colloid Interface Sci.*, 2017, **490**, 279–286.
53 C. Po, Z. Ke, A. Y.-Y. Tam, H.-F. Chow and V. W.-W. Yam, *Chem.–Eur. J.*, 2013, **19**, 15735–15744.
54 Q. Lin, P.-P. Mao, Y.-Q. Fan, P.-P. Jia, J. Liu, Y.-M. Zhang, H. Yao and T.-B. Wei, *Soft Matter*, 2017, **13**, 7360–7364.